LOW SUBSTRATE TEMPERATURE DEPOSITION OF AMORPHOUS AND MICROCRYSTALLINE SILICON FILMS ON PLASTIC SUBSTRATES BY HOT-WIRE CHEMICAL VAPOR DEPOSITION

P.Alpuim[a], V. Chu[a], J.P. Conde[b]

[a] *INESC, Instituto de Engenharia de Sistemas e Computadores, Rua Alves Redol, 9, 1000 Lisbon, Portugal*

[b] *Department of Materials Engineering, Instituto Superior Tecnico, Av. Rovisco Pais,1049-001 Lisbon, Portugal*

Abstract

Amorphous and microcrystalline silicon films were deposited by radio-frequency plasma enhanced chemical vapor deposition (rf-PECVD) and Hot-wire chemical vapor deposition (HW-CVD) on plastic (polyethylene terephthalate-PET) at 100 ºC and 25 ºC. Structural properties of these films were measured by Raman spectroscopy. Electronic properties were measured by dark conductivity and photoconductivity. For amorphous silicon films deposited by rf-PECVD on PET, photosensitivities of $>10^5$ were obtained at both 100 º C and 25 ºC. For amorphous silicon films deposited by HW-CVD, a photosensitivity of $> 10^5$ was obtained at 100 ºC. Microcrystalline silicon films deposited by HW-CVD at 95% hydrogen dilution show $\sigma_{ph} \sim 10^{-4}\ \Omega^{-1}cm^{-1}$, while maintaining a photosensitivity of $\sim 10^2$ at both 100 ºC and 25 ºC. Microcrystalline silicon films with a large crystalline fraction (> 50%) can be deposited by HW-CVD all the way down to room temperature. All the films showed good adhesion and mechanical stability as neither adhesive nor cohesive failure was observed even when the substrates were bent elastically.

ICAMS 18 manuscript ThP2.4

Contact Author:

Pedro Alpuim, Tel: +351-1-3100237; Fax: 351-1-3145843; Email: palpuim@eniac.inesc.pt

KEYWORDS: A200, C185, M215, P180, P242, P260, R110, T200, T340, PLASTIC, PET.

1. Introduction

HW-CVD has attracted much attention since it was found to produce high quality amorphous (a-Si:H) thin films at growth rates more than one order of magnitude higher than those of rf-PECVD [1,2]. One of the unique properties of the HW technique is the availability of high concentrations of atomic hydrogen during film growth. This feature facilitates the growth of microcrystalline silicon (μc-Si:H) at all temperatures and could also be of key importance in the deposition of device-quality amorphous and microcrystalline films at lower substrate temperatures (T_{sub}). The development of a technology which allows the deposition of device quality films at low substrate temperatures enables the use of new types of substrates, making possible devices and electronics on inexpensive and flexible plastic substrates as well as applications integrating thin film electronics with biological materials [3-10].

The optoelectronic properties of a-Si:H and μc-Si:H deposited by HW and rf-PECVD on glass substrates at low T_{sub} have been studied previously [11]. In the present work, the optoelectronic and structural properties of a-Si:H and μc-Si:H films deposited at low T_{sub} (100 and 25 ºC) on PET (polyethylene terephthalate) using HW-CVD are reported for the first time and compared to those deposited by RF-PECVD on PET. The properties of films deposited on plastic are compared to those of films deposited on glass substrates.

2. Experimental Procedures

For HW deposition, a single tungsten filament coil of 0.5 mm diameter and approximately 7 cm total length was placed 5 cm from the substrate and was resistively heated with a DC power supply. The filament temperature was measured with an optical pyrometer (T_{fil} ~ 2500 ºC) and the pressure was kept constant at 20 mTorr. For the RF deposition, the inter-electrode distance was 3 cm, the density of RF power used was 50 mW/cm^2 (in all but the room temperature depositions where it was

100 mW/cm^2), and the pressure was 100 mTorr. For both the HW and RF depositions, the sum of gas fluxes was kept at around 10 sccm, except for the higher dilutions where it was necessary to increase the flux so that the SiH_4 flux was not less than 0.5 sccm, which was the lower limit for the silane mass flow controller.

Films were deposited on Corning 7059 glass and PET [12]. The PET was covered by a 100 nm thick SiN_x passivation layer. Raman spectra were measured in the backscattering geometry using a Raman microprobe. The power of the incident beam was set below 50 mW to avoid thermally induced crystallization. [13-15].

3. Results

Table 1 summarizes the measured properties of selected films deposited on PET. The Raman spectra of films deposited by rf-PECVD on PET (fig. 1a and fig. 1b) show the dependence of the crystalline fraction on film thickness of samples deposited at substrate temperatures of 100 ºC and 25 ºC. When the film thickness increases from 100 to 300 nm, the crystalline fraction increases from 16 to 40% for the film deposited at T_{sub}=25 ºC and 99% H_2 dilution, and from 12 to 55% for the film deposited at T_{sub}=100 ºC and 98% H_2 dilution. The crystalline fractions of the 300 nm rf films on PET approach those of the corresponding films deposited on glass – 42% for the 25 ºC and 58 % for the 100 ºC sample. The same effect can be observed in the case of the HW film deposited at 25 ºC on PET using 90% hydrogen dilution (Fig. 1c). The crystalline fraction increases from 24% for a 100 nm film to 62% for a 300 nm film, closely matching the 57% value for a 230 nm film deposited on glass using the same deposition conditions.

The Raman spectra in Fig.2 illustrate the amorphous to microcrystalline transition as a result of increasing the hydrogen dilution of silane in films deposited on PET at T_{sub}=25 ºC by rf (fig.2a) and by HW (fig.2b). All samples are 300 nm thick, except the 95% H_2 diluted film by HW which is 100 nm thick. The use of a 100 nm film at this hydrogen dilution is justified by two facts: first, this film

already shows structure and properties comparable with a reference sample on glass; second, at this level of hydrogen dilution the deposition rate is not fast enough (r_d~1 Å/s) to prevent the heating of the substrate beyond room temperature for thicknesses above 100 nm.

Figure 3 shows σ_{ph} (fig. 3a) and σ_d (fig. 3b) of films deposited by HW at substrate temperatures of 100 ºC and 25 ºC on PET. The σ_d of the films deposited on PET is essentially indistinguishable from that of reference films deposited on glass independently of T_{sub} and film thickness. Thick amorphous films (d ≥300 nm) deposited on PET (at 60% H_2 dilution for T_{sub}=100 ºC and at 80% H_2 dilution for T_{sub}=25 ºC, respectively) show σ_{ph} comparable to those of films deposited on glass under the same conditions and with the same thickness. However, when deposited on PET, the electronic properties of these films show a very strong dependence on film thickness resulting in a decrease of σ_{ph} of 1-2 orders of magnitude for a decrease of film thickness from 300 nm to 100 nm. At 90% hydrogen dilution and T_{sub}=25 ºC, σ_d shows transport properties intermediate between typical amorphous and typical microcrystalline values (~10^{-7} $\Omega^{-1}cm^{-1}$). σ_{ph} experiences a fourfold increase when film thickness increases from 100 to 300 nm (from 9.1×10^{-7} $\Omega^{-1}cm^{-1}$ to 3.7×10^{-6} $\Omega^{-1}cm^{-1}$). At T_{sub}=100 ºC the 100 nm film has σ_{ph} (7.6×10^{-6} $\Omega^{-1}cm^{-1}$), one order of magnitude beneath the reference 500 nm films on glass. On the other hand, at higher values of hydrogen dilution (95%), the thin (100 nm) films deposited on PET have higher σ_{ph} than the thick (500 nm) reference films on glass without a corresponding increase in σ_d.

4. Discussion

a-Si:H and μc-Si:H films were deposited on PET at T_{sub}=25 ºC and T_{sub}=100 ºC with good adhesion and mechanical stability. Small deformations applied to the substrate within its elastic limit cause no apparent damage to the films.

Both Raman and conductivity data indicate a strong thickness dependence of structure and optoelectronic properties in all HW films except in those where high hydrogen dilution (95%) was used. This dependence, already observed in amorphous HW films on glass deposited at the same temperatures (although not observed for $T_{sub}\geq 220$ ºC [16]) and in microcrystalline HW films (although in much thinner films, in the 10 nm range) on glass, becomes more pronounced in the case of deposition on PET. rf amorphous films show no thickness dependence of their properties while microcrystalline films again show that effect, in particular films deposited at the onset of the amorphous to microcrystalline transition. This is particularly evident for the T_{sub}=100 ºC and 98% H_2 dilution film (see table 1) where $\sigma_d \sim 10^{-11}$ $\Omega^{-1}cm^{-1}$ for the 100 nm film, indicating conduction through a dominant amorphous tissue, while $\sigma_d \sim 5.10^{-6}$ $\Omega^{-1}cm^{-1}$ for the 300 nm film is more characteristic of microcrystalline transport. This thickness dependence can have implications in the design of devices incorporating these films.

The use of hydrogen dilution, both in rf and HW, allows the deposition of films on PET with improved optoelectronic properties that are comparable to those deposited on glass using the same deposition conditions, provided that the thickness dependence is taken into account. Of particular importance are the microcrystalline films by HW deposited with 95% hydrogen dilution where the large supply of atomic hydrogen to the surface of the growing film seems to be enough to overcome the thickness dependence and allows films to be produced which have higher σ_{ph} and the same σ_d as reference films on glass substrates. The very different character of the amorphous to microcrystalline transition in rf (abrupt) and HW (gradual) observed in films deposited on glass [11] is confirmed here for films deposited on PET. The values of hydrogen dilution at which the amorphous to microcrystalline transition occurs in rf for T_{sub}=25 ºC and T_{sub}=100 ºC is the same for films deposited on PET and on glass .

5. Conclusions

Amorphous and microcrystalline silicon films were deposited at 100 ºC and 25 ºC on PET with electronic and structural properties comparable to those of corresponding reference films grown on glass using the same deposition conditions. These films showed good adhesion to the plastic substrate.

At low temperatures ($T_{sub} \leq$ 100 ºC), the photosensitivity (σ_{ph}/σ_d) of amorphous films deposited by HW is highly dependent on the film thickness. An increase of 1-2 orders of the photosensitivity is observed when the thickness is increased from 100 nm to 300 nm.

For low temperature (<100ºC) deposition on PET, rf-PECVD is preferable for amorphous films, but HW-CVD shows more promise in the deposition of microcrystalline silicon.

Acknowledgements

The authors thank R. Almeida and I. Nogueira (ICEMS) for the use of the Raman equipment. This work was supported by the Fundação para a Ciência e Tecnologia (FCT) with Pluriannual Contracts with UCES/ICEMS (IST) and INESC and by projects PRAXIS/3/3.1/MMA/1775/95 and PRAXIS/3/3.1/MMA/1792/95. One of the authors (P. Alpuim) thanks the Department of Physics of University of Minho for a leave of absence and the *Fundação Luso-Americana para o Desenvolvimento* for a travel grant.

References

[1] H. Matsumura, Jpn. J. Appl. Phys., Part 2, 25 (1986) L949.

[2] J.P. Conde, P. Brogueira, and V. Chu, Phil. Mag. B 76 (1997) 299.

[3] Y. Hishikawa, S. Tsuge, N. Nakamura, S. Tsuda, S. Takano, and Y. Kuwano, J. Appl. Phys. 69 (1991) 508.

[4] P. Roca i Cabarrocas, Appl. Phys. Lett. 65 (1994)1674.

[5] M.K. Cheung and M.A. Petrich, J. Appl. Phys. 73 (3237) 1993.

[6] E. Srinivasan, D.A. Lloyd, and G.N. Parsons, J. Vac. Sci. Technol. A 15 (1997) 77.

[7] M.S. Feng, C.W. Liang, and D. Tseng, J. Electrochem. Soc. 141 (1994) 1040.

[8] C.S. McCormick, C.E. Weber, and J.R. Abelson, J. Vac. Sci. Technol. A 15 (1997) 2770.

[9] S.M. Gates, Mat. Res. Soc. Symp. Proc. 467 (1997) 843.

[10] H. Gleskova, S. Wagner, Z. Suo, Mat. Res. Soc. Symp. Proc. 507 (1998) .

[11] P. Alpuim, V. Chu, and J.P. Conde, J. Appl. Phys, to be published (October 1999).

[12] from Goodfellow Cambridge Limited.

[13] M. Vanacek, J. Kocka, J. Strichlik, Z. Kosicek, O. Stika, and A. Triska, Sol. Energy. Mater. 8 (1983) 411.

[14] T. Kaneko, M. Wakagi, K. Onisawa, and T. Minemura, Appl. Phys. Lett. 64 (1994) 1865.

[15] S. Veprek, F.A. Sarott, and Z. Iqbal, Phys. Rev. B 36 (1987) 3344.

[16] J.P. Conde, H. Silva, V. Chu, Mat. Res. Soc. Symp. Proc. 507 (1998) 909.

Figure captions

Figure 1 Raman spectra for (a) rf on PET deposited using 98% hydrogen dilution at T_{sub}=100 ºC; (b) rf on PET using 99% hydrogen dilution at T_{sub}=25 ºC; (c) HW on PET using 90% hydrogen dilution at T_{sub}=25 ºC. In all the plots the Raman spectrum for a reference film deposited on a glass substrate is shown for comparison.

Figure 2 Raman spectra showing the amorphous to microcrystalline transition for rf and HW deposited films at T_{sub}=25 ºC on PET.

Figure 3 (a) Photoconductivity (at a carrier generation rate of 10^{21} $cm^{-3}s^{-1}$) and (b) dark conductivity of HW deposited films as a function of hydrogen dilution. The dark (-) and photoconductivities (+) of films grown on glass substrates at T_{sub}=100 ºC (continuous line) and at T_{sub}=25 ºC (dashed line) are shown for comparison. The arrows point out the increase in σ_{ph} and σ_d when the thickness of the film is increased from 0.1 μm (thin) to 0.3 μm (thick).

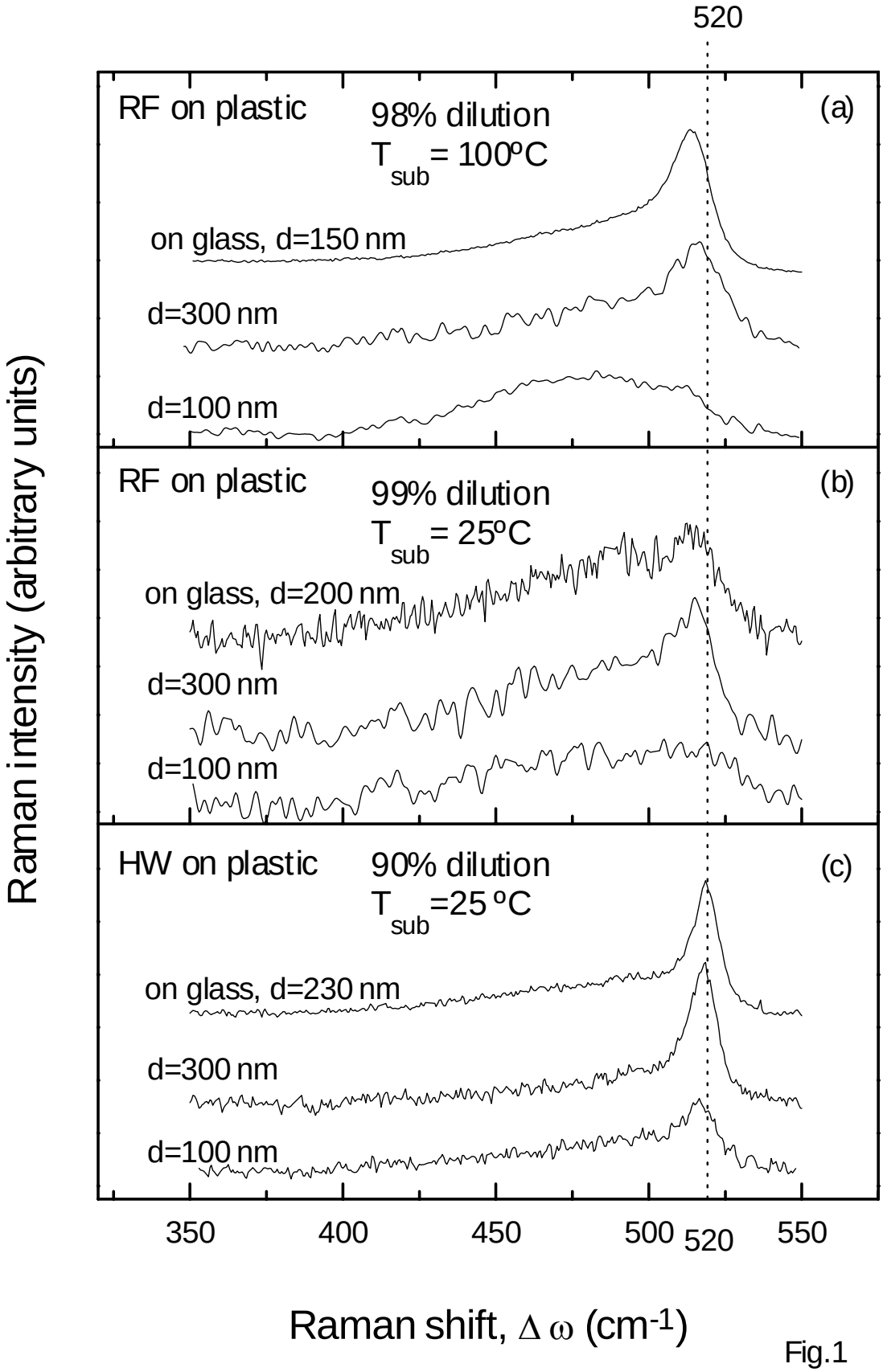
520
RF on plastic
98% dilution
T sub = 100ºC
(a)
on glass, d=150 nm
d=300 nm
d=100 nm
RF on plastic
99% dilution
T sub = 25ºC
(b)
on glass, d=200 nm
d=300 nm
d=100 nm
HW on plastic
90% dilution
T sub =25 ºC
(c)
on glass, d=230 nm
d=300 nm
d=100 nm
350
400
450
500
520
550
Raman intensity (arbitrary units)
Raman shift, Δ ω (cm-1)

Fig.1

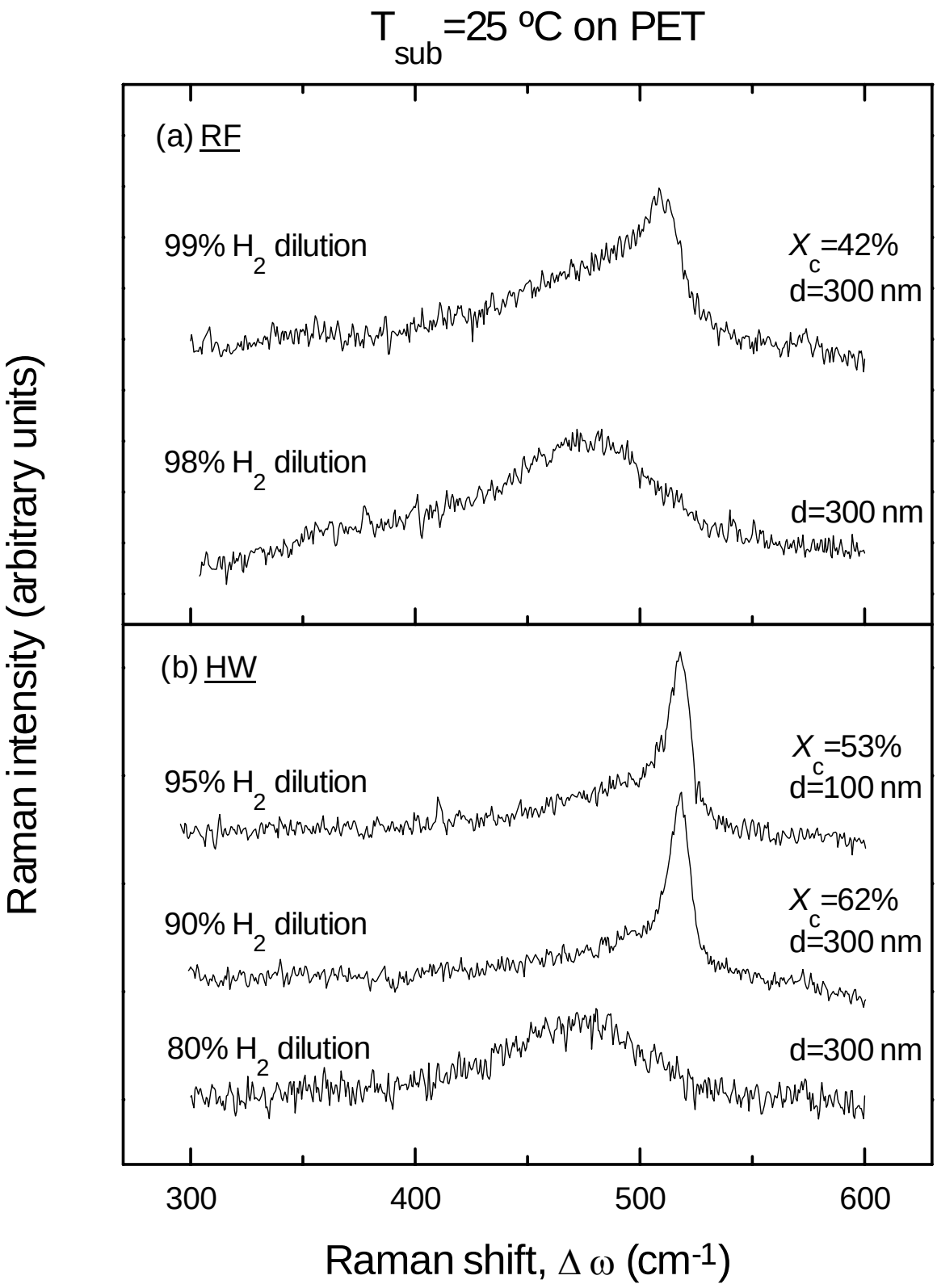
T sub =25 ºC on PET
(a) RF
99% H2 dilution
Xc =42%
d=300 nm
98% H2 dilution
d=300 nm
(b) HW
95% H2 dilution
Xc =53%
d=100 nm
90% H2 dilution
Xc =62%
d=300 nm
80% H2 dilution
d=300 nm
300
400
500
600
Raman shift, Δ ω (cm-1)
Raman intensity (arbitrary units)

Fig.2

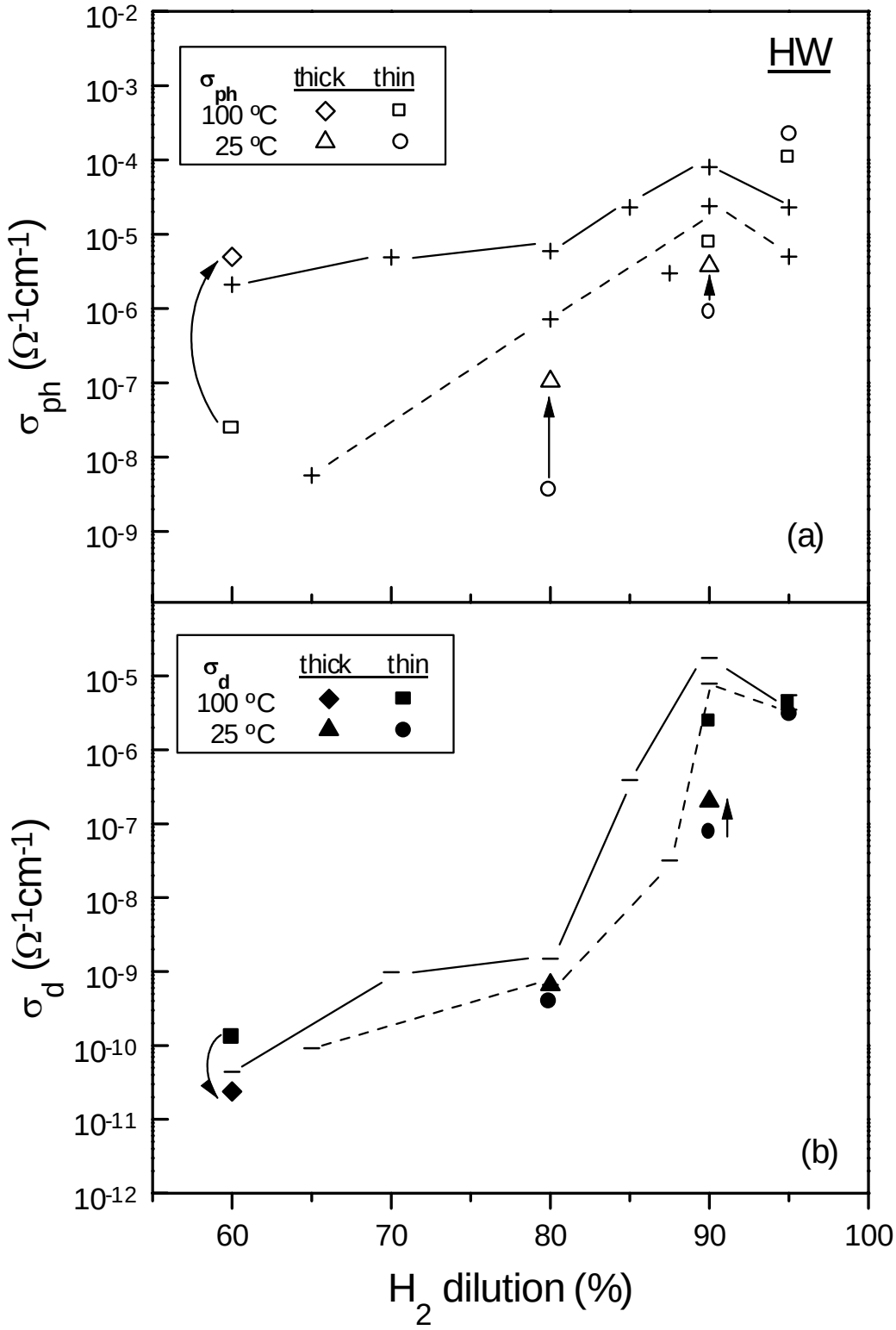
HW
σph
thick thin
100 ºC
25 ºC
σph (Ω-1cm-1)
(a)
σd
thick thin
100 ºC
25 ºC
σd (Ω-1cm-1)
(b)
H2 dilution (%)

Fig.3

TABLE 1: Properties of films deposited on plastic

CVD techn.	T_{sub} (ºC)	sample	H_2 (%)	d (μm)	σ_d ($\Omega^{-1}cm^{-1}$)	E_a (eV)	σ_{ph} ($\Omega^{-1}cm^{-1}$)	γ	X_c (%)
RF	100 ºC	S1486	96	0.1	$1.0x10^{-10}$	0.87	$3.4x10^{-6}$	0.81	0
		S1520	98	0.3	$3.8x10^{-6}$	0.4	$2.2x10^{-5}$	0.43	55
		S1487	98	0.1	$1.4x10^{-11}$	0.9	$1.5x10^{-7}$	0.80	12
	25 ºC	S1493	98	0.1	$1.9x10^{-11}$	0.43	$2.0x10^{-7}$	0.78	0
		S1518	99	0.3	$6.3x10^{-9}$	0.66	$2.9x10^{-7}$	0.58	42
		S1489	99	0.1	$1.1x10^{-9}$	0.57	$6.2x10^{-8}$	0.56	16
HW	100 ºC	S1501	60	1.0	$2.4x10^{-11}$	0.55	$5.0x10^{-6}$	0.80	0
		S1488	60	0.1	$1.3x10^{-10}$	0.85	$2.4x10^{-8}$	0.79	0
		S1498	90	0.1	$2.5x10^{-6}$	0.56	$7.6x10^{-6}$	0.67	79
		S1525	95	0.1	$4.3x10^{-6}$	0.51	$1.1x10^{-4}$	0.92	75
	25 ºC	S1515	80	0.3	$6.9x10^{-10}$	0.74	$1.1x10^{-7}$	0.85	0
		S1494	80	0.1	$3.8x10^{-10}$	0.65	$3.5x10^{-9}$	0.94	0
		S1519	90	0.3	$2.0x10^{-7}$	0.68	$3.7x10^{-6}$	0.57	62
		S1490	90	0.1	$7.4x10^{-8}$	0.65	$9.1x10^{-7}$	0.50	24
		S1516	95	0.1	$3.0x10^{-6}$	0.67	$2.2x10^{-4}$	0.64	53